Int. J. Heat Mass Transfer. Vol. 29, No. 10, pp. 1585–1592, 1986
Printed in Great Britain

0017-9310/86 $3.00 + 0.00

Heat transport in a turbulent plane wake

R. A. ANTONIA and L. W. B. BROWNE
Department of Mechanical Engineering, University of Newcastle, N.S.W. 2308, Australia

(*Received* 18 *December* 1985 *and in final form* 8 *May* 1986)

Abstract—Measurements are presented for the budgets of the average longitudinal and lateral heat fluxes in the self-preserving region of a turbulent plane wake. Using these measurements and a time scale based on the temperature variance and the average temperature dissipation, numerical values are proposed for the constants that appear in currently used models for the temperature–pressure gradient interaction. Except in the outer intermittent region, the lateral heat flux is related in a simple way to the lateral Reynolds shear stress. This simple relation is emphasised when only the turbulent flow zones are considered.

INTRODUCTION

IT IS WELL recognised that the ability to predict the rate of transport of momentum and heat in turbulent shear flows is important for many practical applications. There is also increasing evidence to indicate that a significant portion of this transport is carried by spatially coherent structures whose degrees of organisation, strength and other characteristics may vary from flow to flow. Whilst prediction of the transport of momentum and heat or mass on the basis of these structures remains a worthwhile objective for the future, turbulence modelling based on the time-averaged Navier–Stokes equations continues to meet an important need. Within the framework of turbulence modelling, it is generally accepted that the use of Reynolds stress transport equations is preferable to the use of eddy viscosity models. Analogously, transport equations for the time-averaged heat fluxes have been shown to be of greater validity than eddy diffusivity models.

Second-order, single-point closure models for calculating average fluxes of passive scalar quantities have received significant attention [1, 2]. In the transport equations for $\overline{u\theta}$ and $\overline{v\theta}$, the average longitudinal and lateral heat fluxes, respectively, the correlation between the temperature fluctuation and the gradient (in either x or y) of the pressure fluctuation represents an important contribution and is of the same order as the production terms in the equations. Various models, e.g. [3–5], have been proposed for this correlation. The majority of these models have been applied to situations where temperature is a passive marker of the flow, but there have also been applications, e.g. [6], to the convective planetary boundary layer where buoyancy effects are dominant. It is true, as has been pointed out by Launder [3], that an accurate prediction of the scalar field depends largely on the ability to predict the velocity field accurately. It is nevertheless also true that terms in the transport equations for the heat fluxes are relatively more accessible to measurement than those in transport equations for the Reynolds stresses. In particular all terms in the transport equation for $\overline{\theta^2}$, which together with a transport equation for the temperature dissipation provides a turbulence time scale for the thermal field, can be measured. By contrast, the assumption of isotropy is usually made in evaluating the turbulent energy dissipation, the pressure diffusion term being inferred by difference.

Since the various proposals for the temperature–pressure gradient correlation involve a number of constants, it is desirable that the latter be determined directly by experiment. Applications of existing models have often, although not always, selected the constants by optimising agreement of the computed results with experiment. It has also been noted [3, 7] that the constants can vary considerably between different flows.

In a previous paper [7], constants that appear in models of the temperature–pressure gradient correlation were directly inferred from measurements in a classical turbulent flow: a plane jet into still air. In this paper, we present measurements of the budgets of the heat fluxes $\overline{u\theta}$ and $\overline{v\theta}$ in another classical flow: the wake of a circular cylinder developing with zero mean pressure gradient. Except for the temperature–pressure gradient correlations which were obtained by difference, all terms in the transport equations for $\overline{u\theta}$ and $\overline{v\theta}$ were measured at three stations in the self-preserving region of the flow. Since detailed measurements of these terms were made in a similar flow by Fabris [8–11] at primarily one station in the self-preserving flow region, a comparison is made, whenever possible, between the present measurements and those of Fabris. We also consider non-dimensional structural parameters associated with the turbulence structure which may be of use in parameterising heat transport. The existence of intermittency is taken into account by presenting conditionally sampled measurements in the outer part of the wake.

NOMENCLATURE

a_θ structural parameter for the thermal field, defined in equation (11)
b_θ structural parameter for the thermal field, defined in equation (10)
$c_{1\theta}, c_{2\theta}$ non-dimensional constants in equations (8) and (9)
d outer diameter of wake-generating tube [m]
L y value at half-maximum velocity defect point [m]
N average dissipation of $\overline{\theta^2}/2$, defined as $\alpha[\overline{(\partial\theta/\partial x)^2} + \overline{(\partial\theta/\partial y)^2} + \overline{(\partial\theta/\partial z)^2}]$ [$^\circ C^2\,s^{-1}$]
p kinematic pressure fluctuation [$m^2\,s^{-2}$]
T_0 maximum (centreline) mean temperature, relative to ambient [°C]
$\bar{T}$ mean temperature, relative to ambient [°C]
$\overline{u\theta}$ average (thermometric) longitudinal heat flux [$m\,s^{-1}\,^\circ C$]
U_0 maximum (centreline) velocity defect [$m\,s^{-1}$]
$\bar{U}$ mean velocity in x direction [$m\,s^{-1}$]
u, v, w velocity fluctuations in x, y and z directions [$m\,s^{-1}$]
$\overline{v\theta}$ average (thermometric) lateral heat flux [$m\,s^{-1\,\circ}C$]
x longitudinal direction, cf. Fig. 1 [m]
x_0 effective or virtual origin, equations (5)–(7), equal to $-125d$ [m]
y in direction of main shear, cf. Fig. 1 [m].

Greek symbols

α molecular thermal diffusivity [$m^2\,s^{-1}$]
ε average turbulent energy dissipation [$m^2\,s^{-3}$]
η non-dimensional distance, y/L
θ temperature fluctuation, $\bar{\theta} \equiv 0$ [°C]
$\overline{\theta^2}$ temperature variance [$^\circ C^2$]
λ Taylor microscale, $\overline{u^2}^{1/2}/\overline{(\partial u/\partial x)^2}^{1/2}$ [m]
ν kinematic viscosity [$m^2\,s^{-1}$]
ρ correlation coefficient between velocity and/or temperature fluctuations, e.g. $\rho_{u\theta} = \overline{u\theta}/(\overline{u^2}^{1/2}\overline{\theta^2}^{1/2})$
τ_θ time scale for thermal field [$\overline{\theta^2}/2N$]
τ'_θ time scale for thermal field [$\overline{\theta^2}/2N_{iso}$].

Subscripts

0 conditions at the wake centreline
1 free-stream conditions
t refers to quantities in only the turbulent flow region.

EXPERIMENTAL DETAILS

The wake was generated by a stainless-steel tube of outer diameter (d) of 2.67 mm, mounted horizontally in the mid-plane of the working section (350 × 350 mm, 2.4 m long) of a non-return, blower-type wind tunnel. The tube was placed at a distance of 20 cm downstream from the beginning of the working section. Measurements were made at a free-stream velocity U_1 of 6.7 $m\,s^{-1}$ (Reynolds number $U_1 d/\nu$ = 1170) and zero pressure gradient, the latter achieved by slightly tilting the floor of the working section. The tube was electrically heated ($\simeq$ 100 W) to provide a passive marking of the flow by temperature at sufficiently large distances from the tube (at x/d = 420, $T_0 \simeq 0.82^\circ C$). Detailed measurements of various turbulence quantities were made at three streamwise stations: x/d = 273, 420 and 600 (the co-ordinates used are shown in Fig. 1).

Velocity fluctuations u and v were obtained with a ×-wire, mounted in the x–y plane and comprising Pt–10%Rh Wollaston wires (diameter = 5 μm, length $\simeq$ 0.9 mm) separated by about 0.9 mm in the spanwise z direction. The temperature fluctuation θ was measured with a cold wire (Pt–10%Rh, diameter = 0.63 μm, length $\simeq$ 1 mm) placed about 0.5 mm in front of the wire crossing point of the ×-probe. The hot wires were operated with DISA 55M10 constant temperature anemometers at an overheat ratio of 0.8. The cold wire was operated with an in-house constant current circuit supplying 0.1 mA.

The instantaneous voltages from the constant temperature and constant current anemometers were first filtered (2000 Hz), after applying appropriate

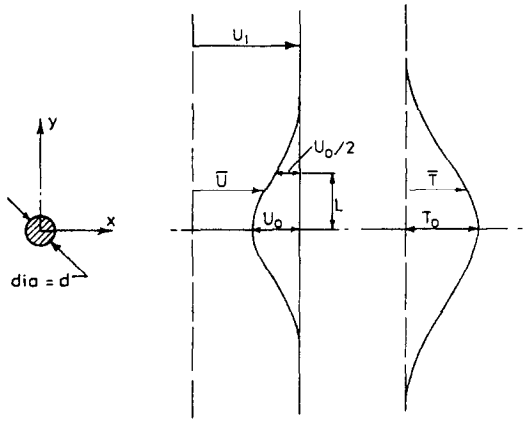

FIG. 1. Definition sketch.

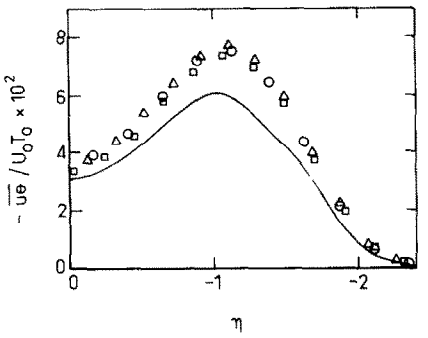

FIG. 2. Average longitudinal heat flux distributions. △ $x/d = 273$; ○ 420; □ 600; —— Fabris [9].

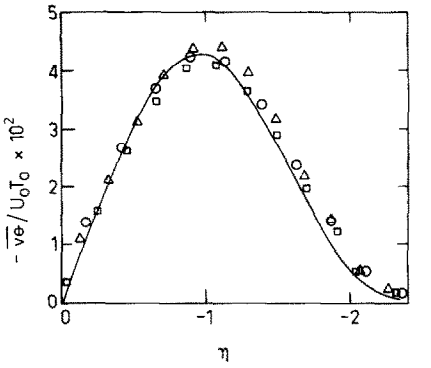

FIG. 3. Average lateral heat flux distributions. Symbols are as in Fig. 2.

gains and offsets, and then sampled (4000 Hz) directly into a computer using an 11 bit plus sign A–D converter. Mean voltages from the anemometers were determined using a small data logging system operating at a sampling frequency of 10 Hz. This data logger was also used for calibrating the wires. Using the calibration constants of the wires, the digitised voltages were converted into digital time series for velocity and temperature.

TRANSPORT EQUATIONS FOR HEAT FLUXES—RESULTS

For a two-dimensional, small-deficit wake, the mean momentum and mean enthalpy equations can be approximated to

$$U_1\frac{\partial}{\partial x}(U_1-\bar{U})-\frac{\partial}{\partial y}\overline{uv}=0 \tag{1}$$

and

$$U_1\frac{\partial\bar{T}}{\partial x}+\frac{\partial\overline{v\theta}}{\partial y}=0. \tag{2}$$

Using the same order of approximation for (1) and (2), transport equations for the heat fluxes $\overline{u\theta}$ and $\overline{v\theta}$, written originally by Corrsin [12] in tensorial form, reduce to

$$U_1\frac{\partial}{\partial x}\overline{u\theta}+\underbrace{\overline{uv}\frac{\partial\bar{T}}{\partial y}+\overline{v\theta}\frac{\partial\bar{U}}{\partial y}}_{\text{production}}+\underbrace{\frac{\partial}{\partial y}(\overline{uv\theta})}_{\text{diffusion}}+\underbrace{\theta\overline{\frac{\partial p}{\partial x}}}_{\text{dissipation}}=0 \tag{3}$$

advection

$$U_1\frac{\partial}{\partial x}\overline{v\theta}+\overline{v^2}\frac{\partial\bar{T}}{\partial y}+\frac{\partial}{\partial y}(\overline{v^2\theta})+\theta\overline{\frac{\partial p}{\partial y}}=0. \tag{4}$$

advection production diffusion dissipation

Before considering collectively all the terms in (3) and (4) we turn our attention to the behaviour, across the wake, of the average heat fluxes $\overline{u\theta}$ and $\overline{v\theta}$ and the behaviour of the correlations $\overline{uv\theta}$ and $\overline{v^2\theta}$, the gradients of which represent the diffusion terms.

The distributions in Figs. 2 and 3 of $\overline{u\theta}$ and $\overline{v\theta}$, normalised by the self-preserving scales U_0, T_0 and plotted in terms of the non-dimensional co-ordinate η, underline the good support for self-preservation for the range of x/d covered by the experiments. Fabris' [8, 10] data at $x/d = 420$, are generally in closer agreement with the present $\overline{v\theta}/U_0T_0$ than with the $\overline{u\theta}/U_0T_0$ distributions. Note that for the region $y > 0$, the gradients $\partial\bar{U}/\partial y$ and $\partial\bar{T}/\partial y$ are positive and negative, respectively, while the correlations $\overline{u\theta}, \overline{v\theta}, \overline{uv}$ are negative, positive and positive, respectively. For $y < 0$, $\partial\bar{U}/\partial y$, $\partial\bar{T}/\partial y$ and $\overline{v\theta}$ change sign. Our detailed measurements were made for $y < 0$ although symmetry about $y = 0$ was first verified. Fabris also verified symmetry so we were able to compare his $y > 0$ results directly with our $y < 0$ results.

The normalised third-order transport correlations $\overline{uv\theta}/U_0^2T_0$ and $\overline{v^2\theta}/U_0^2T_0$, which were first obtained by Fabris [8, 9, 11], are plotted in Figs. 4 and 5, respectively. Apart from supporting self-preservation, the present distributions, especially in the case of $\overline{v^2\theta}$, are in good agreement with those of Fabris. Whereas $\overline{v^2\theta}$ is symmetrical about $\eta = 0$, $\overline{uv\theta}$ is antisymmetrical and indicates a change of sign at $\eta \simeq -0.8$. This change of sign is most simply explained if, as suggested by Fabris, the correlation is viewed as a lateral transport of $\overline{u\theta}$. The negative values of $\overline{uv\theta}$ near the centreline reflect the inward transport of $\overline{u\theta}$ away from

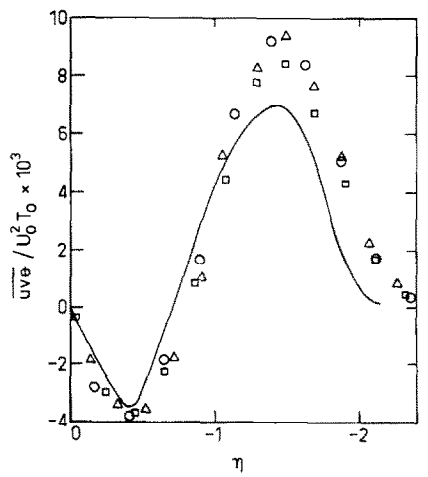

FIG. 4. Correlation $\overline{uv\theta}/U_0^2T_0$. Symbols are as in Fig. 2.

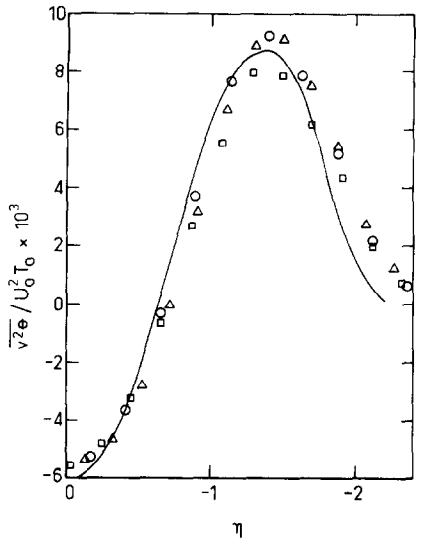

FIG. 5. Correlation $\overline{v^2\theta}/U_0^2T_0$. Symbols are as in Fig. 2.

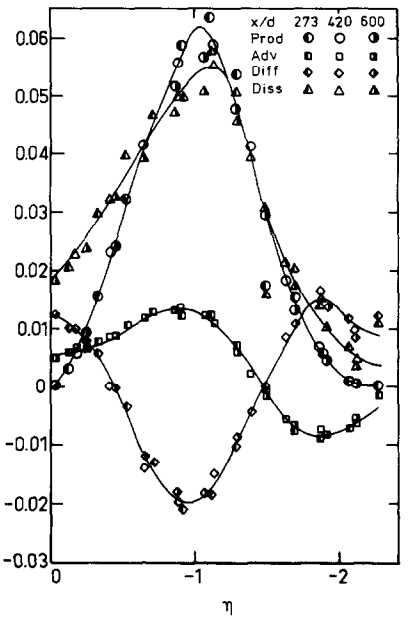

FIG. 6. Budget of average longitudinal heat flux. Solid curves are hand best fits.

the location of maximum $|\overline{u\theta}|$, the positive values of $\overline{uv\theta}$ in the outer wake region then reflecting the outward transport of $\overline{u\theta}$ away from the maximum $|\overline{u\theta}|$ location. A similar shape for $\overline{uv\theta}$ was obtained for a plane jet into still air [7] where it was shown that a gradient-diffusion model is qualitatively, although not quantitatively, applicable.

Terms in equations (3) and (4) that involve differentiation with respect to y were evaluated by first applying least-square fits to the relevant distributions and then numerically differentiating these fits. Least-square fits were applied to the estimates for the derivatives. The advection terms in (3) and (4) involve differentiation with respect to x and were inferred from derivatives with respect to η, e.g. $\partial\overline{v\theta}/\partial x = \partial/\partial\eta(\overline{v\theta})\cdot\partial\eta/\partial L\cdot\partial L/\partial x$, using the experimentally verified assumption of self-preservation and the measured streamwise evolutions of U_0, T_0 and L, namely

$$\frac{U_0}{U_1} = 1.28\left(\frac{x-x_0}{d}\right)^{-1/2} \tag{5}$$

$$\frac{T_0}{T_c} = 23.3\left(\frac{x-x_0}{d}\right)^{-1/2} \tag{6}$$

$$\frac{L}{d} = 0.20\left(\frac{x-x_0}{d}\right)^{1/2}. \tag{7}$$

The value of x_0 was $-125d$ and in equation (6), the normalising temperature T_c is the value of T_0 ($= 0.82°C$) at $x/d = 420$. The various terms in equations (3) and (4) have been normalised by multiplying by $(L/U_0^2T_0)$ and are plotted in Figs. 6 and 7. The terms are shown at each of the three stations although it would clearly have been sufficient, in the light of Figs. 6 and 7 and the previous figures, to have used a single distribution for each of the terms. The solid curves in Figs. 6 and 7 are shown mainly to clarify the distinction between the various terms. Comparison with Fabris is not made in these figures as we did not have information corresponding to equations (5)–(7) for Fabris' experiments. It is nevertheless reasonable to expect, on the basis of Figs. 2–5, good qualitative agreement between the present

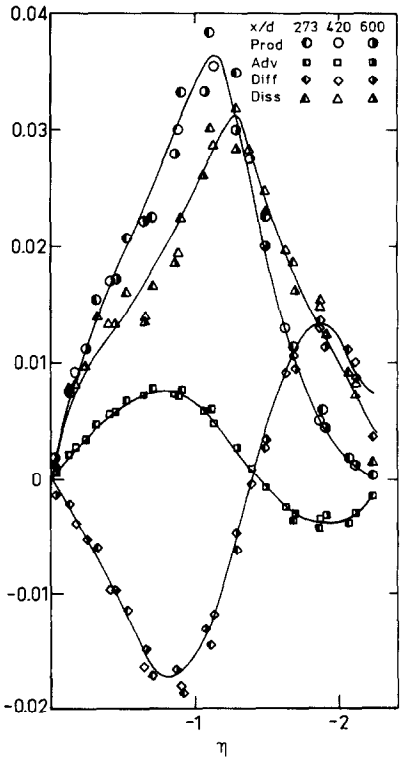

FIG. 7. Budget of average lateral heat flux. Solid curves are hand best fits.

heat flux budgets and those that could be inferred from Fabris' data.

The budgets of $\overline{u\theta}$ (Fig. 6) and $\overline{v\theta}$ (Fig. 7) have generally similar appearances except near the centreline. For the $\overline{u\theta}$ budget, there is a gain of $\overline{u\theta}$ as a result of advection and especially diffusion at or near $\eta = 0$. Since the production term is zero at $\eta = 0$, the sum of the advection and diffusion terms is balanced by the temperature–pressure gradient correlation. Note that the quantities $-(L/U_0^2T_0)\overline{\theta\partial p/\partial x}$ and $-(L/U_0^2T_0)\overline{\theta\partial p/\partial y}$, which are equal to the sum of the first three terms on the left-hand sides of equations (3) and (4), are plotted in Figs. 6 and 7, respectively. It is clear from these figures that the dissipation (destruction or scrambling) is of comparable magnitude to the production almost everywhere across the wake.

All models for the temperature–pressure gradient correlation or, more correctly, the pressure–temperature gradient correlation, involve a time scale for the turbulence. The latter is usually identified with the ratio $\overline{q^2}/2\varepsilon$ where $\overline{q^2}/2$ is the turbulent kinetic energy and ε is the average dissipation corresponding to $\overline{q^2}/2$. It has also been proposed that the time scale in the model should contain some weighting from the time scale of the thermal field. An obvious choice for this latter time scale is $\overline{\theta^2}/2N$. The advantage of such a choice is that all three components of N can be measured. Measurements of N in different shear flows (e.g. [13–16]) including the present one [17] have clearly indicated that N is significantly larger than N_{iso}, the value obtained by assuming local isotropy. In the present flow [17], the ratio N/N_{iso} increases from about 1.5 and $\eta = 0$ to almost 2.0 at the location of maximum temperature variation or dissipation.

Estimates of $\overline{q^2}/2\varepsilon$ have invariably identified ε with ε_{iso}, an assumption which, to date, remains experimentally unverified. The present distribution of $\tau_\theta = \overline{\theta^2}/2N$ is shown in Fig. 8 together with the timescale $\tau'_\theta = \overline{\theta^2}/2N_{iso}$. Apart from the smaller magnitude of τ_θ, the variation of τ_θ across the wake is also smaller than that of τ'_θ. Using the distribution of τ_θ shown in Fig. 8, estimates were made of the constants $c_{1\theta}$ and $c_{2\theta}$ that appear in the models, e.g. [1]

$$\overline{p\frac{\partial\theta}{\partial x}} = -c_{1\theta}\frac{\overline{u\theta}}{\tau_\theta} + c_{2\theta}\overline{v\theta}\frac{\partial\bar{U}}{\partial y} \tag{8}$$

and

$$\overline{p\frac{\partial\theta}{\partial y}} \simeq -c_{1\theta}\frac{\overline{v\theta}}{\tau_\theta} + c_{2\theta}\overline{v\theta}\frac{\partial\bar{V}}{\partial y}. \tag{9}$$

The first of the terms on the right-hand sides of (8) and (9) represents the effect of turbulence interactions only while the second term reflects the presence of mean strain rates. The possible influence of $\partial\bar{T}/\partial y$, as considered, for example, by Dakos and Gibson [5], has been ignored here. The term in (9), $c_{2\theta}\overline{v\theta}(\partial\bar{V}/\partial y)$ where $\bar{V}$ is the mean lateral velocity, is negligibly small. When applying (8) to the experimental data, $\overline{p(\partial\theta/\partial x)}$ was identified with $-\overline{\theta(\partial p/\partial x)}$ (obtained from Fig. 6) since an order of magnitude argument can clearly show that $\partial\overline{p\theta}/\partial x$ is at least one order smaller than the terms that were retained in equations (3) and (4). A least-squares, multiple linear regression was applied to the experimental data to obtain $c_{1\theta}$ and $c_{2\theta}$ using equation (8). The fit obtained is shown in Fig. 9 and the values obtained for the constants were: $c_{1\theta} = 0.86$; $c_{2\theta} = 0.60$. Jones and Musonge [2] obtained, from free shear flow data, a value of 1.0 for $c_{1\theta}$, while Antonia [7] obtained about 2.3 for a jet in still air, using the measured value of N. Using $c_{1\theta} = 0.86$, the values of $\overline{p(\partial\theta/\partial y)}$ calculated using equation (9) were about 60% of the $-\overline{\theta\partial p/\partial y}$ values obtained from Fig. 7. It is possible that this difference reflects the inaccuracy of assuming $\partial/\partial y(\overline{p\theta})$ negligible. As noted earlier, Launder and Samaraweera [1] applied a second-moment turbulence closure for calculating the heat transport in a turbulent wake. A discussion of the results obtained by these authors in the context of the present experiment seems unwarranted in view of the limited data available to

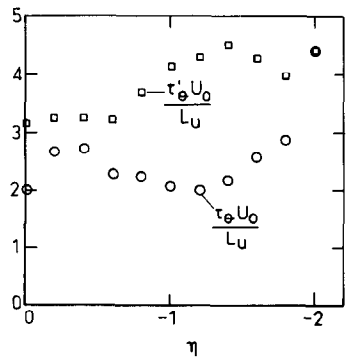

FIG. 8. Distribution of the time scale based on the average dissipation of temperature. ○ $\tau_\theta U_0/L$; □ $\tau'_\theta U_0/L$.

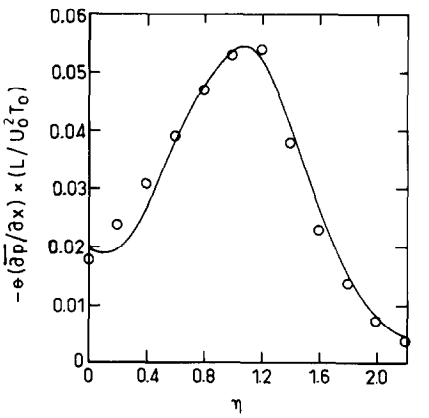

FIG. 9. Best fit to experimental values of $-\overline{\theta(\partial p/\partial x)}$. ○ Experiment; —— least squares fit to equation (8) with $c_{1\theta} = 0.86$ and $c_{2\theta} = 0.60$.

these authors and the limited agreement between calculated and measured Reynolds shear stress distributions.

A FEW TURBULENCE STRUCTURE PARAMETERS

It is of interest to consider the variation across the wake of non-dimensional quantities related directly to the turbulence structure of this flow. One such quantity, shown in Fig. 10, is the ratio $\overline{u\theta}/\overline{v\theta}$, considered by Launder and Samaraweera [1] to be insensitive as to whether self-preserving conditions have been established or not. Apart from reflecting the different behaviours of $\overline{u\theta}$ and $\overline{v\theta}$ near the centreline, there is no significant region over which this ratio can be considered as constant. The magnitude of the present ratio is larger than that for Fabris, reflecting the difference in the $\overline{u\theta}$ distributions (Fig. 2) for these two experiments. Interestingly, but perhaps not surprisingly, the ratio of the turbulent zone averaged heat fluxes shows less variation in the intermittent part of the flow (at $\eta = 0.9$, the intermittency factor is about 0.95) than the ratio $\overline{u\theta}/\overline{v\theta}$. Conditioning of velocity and temperature is equal to the ambient temperature. This detection, discussed in more detail in ref. [18], was carried out using the probability density function of temperature. Note that the convention here, as for Fabris, is such that for example

$$\overline{(u\theta)_t} \equiv \overline{(u-\bar{u}_t)(\theta-\bar{\theta}_t)_t}$$

where $\bar{u}_t$ and $\bar{\theta}_t$ are averages in only the turbulent flow regions.

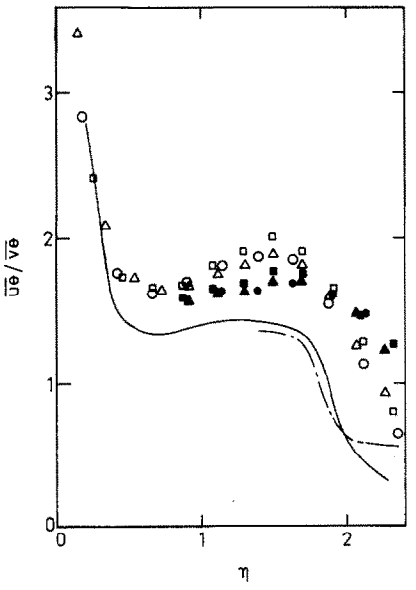

FIG. 10. Ratio of average longitudinal and lateral heat fluxes. Symbols are as in Fig. 2. Open and filled in symbols represent conventional and conditionally turbulent values respectively. Fabris [8]: —— conventional; ——— conditionally turbulent.

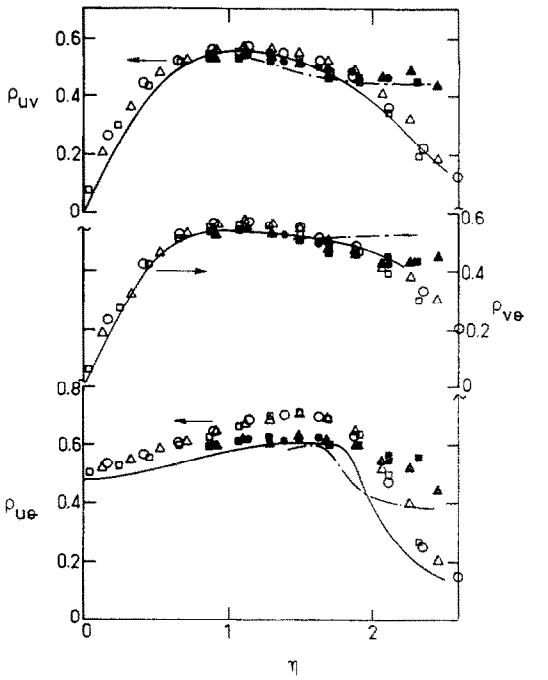

FIG. 11. Correlation coefficients between velocity and temperature fluctuations. Symbols are as in Fig. 10.

Another structure parameter is the correlation coefficient between velocity and/or temperature fluctuations. Conventional and conditional distributions (Fig. 11) of the correlation coefficient between u and v are closely similar with those of the correlation coefficient between v and θ. The similarity between ρ_{uv} and $\rho_{v\theta}$ is emphasised in Fig. 12 where the ratio $\rho_{v\theta}/\rho_{uv}$ is remarkably constant, especially when conditionally turbulent values are considered in the intermittent region of the flow. Saetran [19] observed a similar constancy for $\rho_{v\theta}/\rho_{uv}$ in a slightly heated boundary layer and suggested the following relation (absolute values have been added to make it compatible with the present and other free shear flows)

$$|\overline{v\theta}| = b_\theta |\overline{uv}| \left(\frac{\overline{\theta^2}}{\overline{u^2}}\right)^{1/2}. \qquad (10)$$

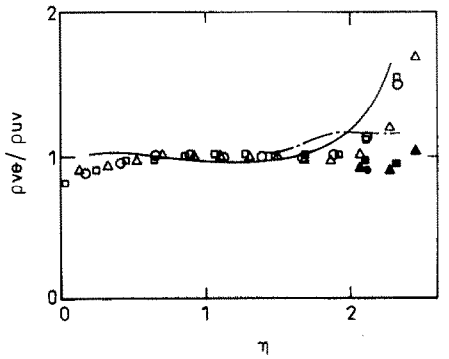

FIG. 12. Ratio of correlation coefficients $\rho_{v\theta}$ and ρ_{uv}. Symbols are as in Fig. 10 (only a few filled symbols are shown for clarity).

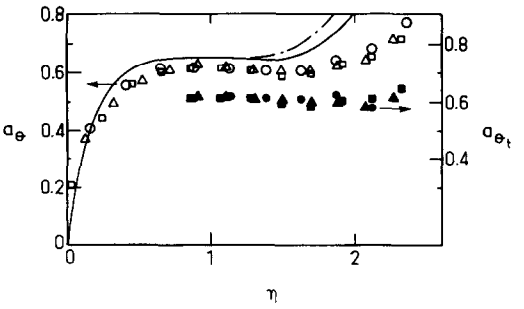

FIG. 13. Structure parameter a_θ. Symbols are as in Fig. 10. Note the different scale for $(a_\theta)_t$.

Saetran obtained a value of 1.15 for b_θ in the boundary layer, whereas a value of 1.0 seems more appropriate for the wake.

Another structural parameter introduced by Bradshaw and Ferriss [20] to transform the transport equation for $\overline{\theta^2}$ into one for $\overline{v\theta}$ is a_θ, defined by

$$a_\theta = \frac{|\overline{v\theta}|}{\overline{\theta^2}^{1/2}|\overline{uv}|^{1/2}} = \frac{|\rho_{v\theta}|}{|\rho_{uv}|^{1/2}}\frac{\overline{v^2}^{1/2}}{\overline{u^2}^{1/2}}. \quad (11)$$

The distribution of a_θ is shown in Fig. 13. Apart from the decrease towards zero near the centreline, there is a significant region for which a_θ is constant, equal to about 0.6. The increase in a_θ in the outer intermittent region becomes less pronounced when only turbulent zone averages (a_{θ_t}) are considered. This is more evident for the present measurements than in Fabris' experiment.

CONCLUSIONS

1. The measured budgets, at three streamwise stations, of the longitudinal and lateral heat fluxes show good support for self-preservation and generally extend the usefulness of Fabris' data from the point of view of turbulence modelling. Except for the magnitude of $\overline{u\theta}$, there is good quantitative agreement between the two experiments.
2. The temperature–pressure gradient correlation is generally comparable to the production term although the contribution by the advection and diffusion terms in the $\overline{u\theta}$ budget cannot be ignored near the centreline. In modelling the correlation, it is important to take into account the anisotropy of the temperature dissipation to estimate the time scale of the turbulence.
3. The close agreement between the correlation coefficients $\rho_{v\theta}$ and ρ_{uv} suggests a relatively simple relation between the lateral heat flux and the Reynolds shear stress in this flow, i.e. $|\overline{v\theta}| = |\overline{uv}|(\overline{\theta^2}/\overline{u^2})^{1/2}$. The structural parameter a_θ is constant over a significant part of the flow.
4. The relatively small variation of conditioned structural parameters in the intermittent region suggests that the prescription of model constants should be simplified when the focus is on only the turbulent flow regions.

Acknowledgement—The support of the Australian Research Group Scheme is gratefully acknowledged.

REFERENCES

1. B. E. Launder and D. S. A. Samaraweera, Application of a second-moment turbulence closure to heat and mass transport in thin shear flows. I. Two-dimensional transport, *Int. J. Heat Mass Transfer* **22**, 1631–1643 (1979).
2. W. P. Jones and P. Musonge, Modelling of scalar transport in homogeneous turbulent flows, *Proc. Fourth Symposium on Turbulent Shear Flows* (Edited by L. J. S. Bradbury, F. Durst, B. E. Launder, F. W. Schmidt and J. H. Whitelaw), Karlsruhe, 17.18–17.24 (1983).
3. B. E. Launder, Heat and mass transport. In *Turbulence—Topics in Applied Physics* (Edited by P. Bradshaw), Vol. 12, pp. 231–287. Springer-Verlag, Berlin (1976).
4. J. L. Lumley, Computational modeling of turbulent flows, *Adv. appl. Mech.* **18**, 123–126 (1978).
5. T. Dakos and M. M. Gibson, On modelling the pressure terms of the scalar flux equations, *Proc. Fifth Symposium on Turbulent Shear Flows* (Edited by L. J. S. Bradbury, F. Durst, B. E. Launder, F. W. Schmidt and J. H. Whitelaw), Cornell University, 12.1–12.6 (1985).
6. C-H. Moeng and J. C. Wyngaard, A study of the closure problem for pressure-scalar covariances, *Proc. Fifth Symposium on Turbulent Shear Flows* (Edited by L. J. S. Bradbury, F. Durst, B. E. Launder, F. W. Schmidt and J. H. Whitelaw), Cornell University, 12.31–12.36 (1985).
7. R. A. Antonia, On a heat transport model for a turbulent plane jet, *Int. J. Heat Mass Transfer* **28**, 1805–1812 (1985).
8. G. Fabris, Conditionally sampled turbulent thermal and velocity fields in the wake of a warm cylinder and its interaction with an equal cool wake. Ph.D. thesis, Illinois Institute of Technology (1974).
9. G. Fabris, Turbulent temperature and thermal flux characteristics in the wake of a cylinder, *Turbulent Shear Flows I* (Edited by F. Durst, B. E. Launder, F. W. Schmidt and J. H. Whitelaw), pp. 55–70. Springer-Verlag, Berlin (1979).
10. G. Fabris, Conditional sampling study of the turbulent wake of a cylinder. Part 1, *J. Fluid Mech.* **94**, 673–709 (1979).
11. G. Fabris, Third-order conditional transport correlations in the two-dimensional turbulent wake, *Physics Fluids* **26**, 422–427 (1983).
12. S. Corrsin, Remarks on turbulent heat transfer: an account of some features of the phenomenon in fully turbulent regions, *Proc. First Iowa Symposium on Thermodynamics*, Iowa, pp. 5–30 (1953).
13. K. R. Sreenivasan, R. A. Antonia and H. Q. Danh, Temperature dissipation fluctuations in a turbulent boundary layer, *Physics Fluids* **20**, 1238–1249 (1977).
14. E. Verollet, Etude d'une couche limite turbulente avec aspiration et chauffage à la paroi. Ph.D. thesis, Université d'Aix-Marseille II (also Rapport CEA-R-4872, C.E.N. Scalay, 1977) (1972).
15. S. Tavoularis and S. Corrsin, Experiments in nearly homogeneous turbulent shear flow with a uniform mean temperature gradient. Part 2. The fine structure, *J. Fluid Mech.* **104**, 349–367 (1981).
16. R. A. Antonia, L. W. B. Browne, A. J. Chambers and S. Rajagopalan, Budget of the temperature variance in a turbulent plane jet, *Int. J. Heat Mass Transfer* **26**, 41–48 (1983).

17. R. A. Antonia and L. W. B. Browne, Anisotropy of the temperature dissipation in a turbulent wake, *J. Fluid Mech.* **163**, 393–403 (1986).
18. R. A. Antonia and L. W. B. Browne, Conventional and conditional Prandtl number in a turbulent plane wake, submitted to *Int. J. Heat Mass Transfer*.
19. L. R. Saetran, Experimental investigation and mathematical modelling of momentum, heat and mass transport in some turbulent flows. Ph.I University of Trondheim (1984).
20. P. Bradshaw and D. H. Ferriss, Calculation of layer development using the turbulent energy IV. Heat transfer with small temperature d Aero Report No. 1271, National Physical La London (1968).

TRANSFERT DE CHALEUR DANS UN JET PLAN TURBULENT

Résumé—On présente des mesures pour le bilan des flux de chaleur moyens longitudinaux et latéraux dan la région de similitude du jet plan turbulent. A partir de ces mesures et d'une échelle de temps basée sur l variance de la température et la dissipation moyenne de la température, des valeurs numériques son proposées pour les constantes qui apparaissent dans les modèles couramment utilisés pour l'interactio pression-gradient de température. Sauf dans la région externe intermittente, le flux thermique latéral es relié de façon simple à la tension latérale de cisaillement de Reynolds. Cette relation simple est mise e valeur lorsque seules les zones turbulentes de l'écoulement sont considérées.

WÄRMETRANSPORT IN EINER TURBULENTEN EBENEN NACHLAUFSTRÖMUNG

Zusammenfassung—Es wurden Messungen über die mittleren längs- und quergerichteten Wärmeströme i dem selbsterhaltenden Gebiet einer turbulenten ebenen Nachlaufströmung vorgestellt. Mit Hilfe diese Messungen und eines Zeitmaßstabes, der auf der Temperaturvarianz und der mittleren Temperatu Dissipation beruht, werden numerische Werte für die Konstanten vorgeschlagen, die in den derzeiti benutzten Modellen für die Wechselwirkung von Temperatur- und Druckgradienten benutzt werde Abgesehen vom äußeren pulsierenden Bereich wurde der quergerichtete Wärmestrom in einfacher Weis in Relation zur quergerichteten Reynolds' schen Schubspannung gesetzt. Diese einfache Beziehun empfiehlt sich, wenn nur turbulente Strömungszonen betrachtet werden.

ТЕПЛОПЕРЕНОС В ТУРБУЛЕНТНОМ ПЛОСКОМ СЛЕДЕ

Аннотация—Измерены значения средних продольных и поперечных тепловых потоков в автом дельной области турбулентного плоского следа. Используя результаты этих измерений масштаб времени, основанный на дисперсии и средней скорости диссипации температурных флу туаций, предложены численные значения констант, входящих в используемые в настоящее врем модели взаимодействия между градиентами температуры и давления. За исключением внешне области перемежающейся турбулентности, поперечный тепловой поток находится в простой зав симости от напряжения Рейнольдса, в особенности в зонах турбулентного течения.